The Ovine Brain as a Model for Human Neurodevelopment: Immunohistochemical Profiling of Brain Maturation Markers in Preterm Lambs

Yoann Rodriguez, Anne Leostic, Olivier Le Coz, Vincent Mauffré, Joanne Fortemps, Lucile Cavarec, Fabienne Constant, Marine Denis, Paul Berveiller, Aude Tessier, et al.

Journal of Comparative Neurology

WILEY

JCN RESEARCH IN SYSTEMS NEUROSCIENCE THE JOURNAL OF COMPARATIVE NEUROLOGY

RESEARCH ARTICLE OPEN ACCESS

The Ovine Brain as a Model for Human Neurodevelopment: Immunohistochemical Profiling of Brain Maturation Markers in Preterm Lambs

Yoann Rodriguez[1,2] | Anne Leostic[1,2,4] | Olivier Le Coz[1,3] | Vincent Mauffré[2,4] | Joanne Fortemps[5] | Lucile Cavarec[2] | Fabienne Constant[2,4] | Marine Denis[2,4] | Paul Berveiller[1,2,6] | Aude Tessier[5] | Olivier Sandra[2,4] | Leslie Schwendimann[7] | Pierre Gressens[7] | François Vialard[8] | Emmanuelle Motte-Signoret, MD, PhD[1,2,9]

[1]Université Paris-Saclay, UVSQ, Inserm, IMPROVE, Versailles, France | [2]Université Paris-Saclay, UVSQ, INRAE, BREED, Jouy-en-Josas, France | [3]Université Paris-Saclay, UMR U1179/UVSQ, Département de Biotechnologie de la Santé, Montigny-Le-Bretonneux, France | [4]Ecole Nationale Vétérinaire d'Alfort, BREED, Maisons-Alfort, France | [5]Poissy St Germain Hospital, Anatomopathology Unit, Poissy, France | [6]Poissy St Germain Hospital, Obstetrics Department, Poissy, France | [7]Université Paris Cité, Inserm, NeuroDiderot, Paris, France | [8]UFR-SVS, UVSQ, Montigny le Bretonneux, France | [9]Poissy St Germain Hospital, Neonatal Intensive Care Unit, Poissy, France

Correspondence: Yoann Rodriguez (yoann.rodriguez@uvsq.fr)

Received: 1 July 2025 | **Revised:** 18 February 2026 | **Accepted:** 2 March 2026

Keywords: preterm birth | brain development | ovine model | immunohistochemical comparison. RRID:NCBITaxon_9940, RRID:AB_2298772, RRID:AB_3107026, RRID:AB_10013382, RRID:AB_839504, RRID:AB_2267671, RRID:AB_94971, RRID:AB_477523, RRID:SCR_018041, RRID:SCR_026521, RRID:AB_2340771, RRID:AB_2340590, RRID:SCR_027461, RRID:SCR_018257, RRID:SCR_001905, RRID:SCR_000432, RRID:SCR_019186, RRID:SCR_027454, RRID:SCR_027455, RRID:SCR_021240

ABSTRACT

Preterm birth is known to severely impact the neurological development of newborns with long-lasting complications and higher risks of neurological disorders. Sheep (*Ovis aries*) is well known as a pre-clinical model in therapeutic studies, such as extra-uterine support. The aim of our study was to investigate the relevance of the lamb as a pre-clinical model for preterm birth when cortical maturation of preterm and term lamb is addressed. Cesarean sections were performed on time-dated pregnant ewes to obtain 13 lambs at 100 days and 140 days of pregnancy each (corresponding to 24 and 36 weeks of pregnancy in humans, respectively). Brains were collected and separated in frontal lobe, temporo-parietal lobe, occipital lobe, and cerebellum. Immunohistochemistry staining was used for each brain area by targeting neurons, interneurons, synaptic vesicles, oligodendrocytes, myelin, astrocytes, and microglia. Quantifications were normalized by the surface area of analysis. Overall, 140-days late preterm lambs have significantly higher mean positivity for interneurons, synaptic vesicles, oligodendrocytes, astrocytes, and myelin than 100-days extremely preterm lambs. Similarly, significantly higher mean positivity for neurons was found in the cerebellum of 140-days term lambs. No significant difference was observed regarding microglia. Based on the cellular and structural markers used in this study, brain development in lamb seems to follow an antero–posterior direction similarly to what was reported in humans. Further studies with more specific markers and in-depth analysis will allow for a more accurate and exhaustive description of brain development in lamb.

1 | Introduction

In humans, preterm birth is defined as birth happening before 37 weeks of pregnancy and represents around 10% of worldwide birth each year, therefore about 15 million (Blencowe et al. 2012; Walani 2020; WHO 2023). Among those, 5% of preterm births are extremely preterm births (< 28 weeks of gestational weeks [GW]) with a reduced survival rate and an increased risk of neurodevelopmental impairment.

From a clinical perspective, extremely preterm infants tend to have lower cognitive score, as well as lower gross and fine motor functions with various severity levels of cerebral palsy, and increased risks of visual and hearing impairment (Adams-Chapman et al. 2018) due to a reduced development of the cortex, lesions of the white matter, a significantly lower cortical surface and grey matter volume, and a higher volume of cerebrospinal fluid (Ajayi-Obe et al. 2000; Inder et al. 2005; Peterson et al. 2000; Volpe 2005).

This impaired neurological development has been shown to also result in long-lasting cognitive complications. Studies following pre-term infants through up to 5 years after birth have shown that while the rate of cerebral palsy decreased and mean intelligence quotient (IQ) increases with GWs (12.4%–2.4% cerebral palsy rate and 89.6–97.3 mean IQ, for children born 24–26 weeks and 32–34 weeks, respectively), there still were significant differences with children born at term (Pierrat et al. 2021). Neurodevelopmental disabilities such as behavioral difficulties and developmental coordination disorders were also more frequent in extremely preterm infants even several years after birth. Those findings correlate with the significantly higher needs of extremely preterm children for educational support and complex developmental interventions to compensate for their disabilities, with up to 60% of children with severe neurodevelopmental disabilities requiring an intervention (Torchin et al. 2015).

More in-depth studies of the impact in neurodevelopment researched cellular and structural alterations that could be resulting from preterm birth by using animal models. Studies on rodents have already shown that inflammation, one of the most frequent factors of preterm birth, leads to the activation of microglia and subsequently reduce the myelinization process (Morin et al. 2022) as well as negatively impacts the development and regulation of interneurons (Stolp et al. 2019) and glial cells (Morin et al. 2022).

Other animal models such as sheep (*Ovis aries*), which is already being used as a model for placental development, metabolic function, and nutrient transport, and has been shown to have many commonalities with human pregnancy (Barry and Anthony 2008) and human neuroanatomy (Banstola and Reynolds 2022), have also been of interest in that regard. Studies have already shown that the lamb's respiratory kinetic and overall weight and size was similar to that of a human child, making the lamb a valid model for research on prematurity. Based on this, studies on therapeutics alternative for preterm birth looked at extrauterine support and were able to demonstrate brain growth and myelination (Partridge et al. 2017) as well as histologic and transcriptomic expression (Cohen et al. 2024) in preterm lamb on extrauterine support similar to same-age term fetal lamb.

While this field of research would most likely profit from using a primate model, due to the inherent resemblance with human beings, the limitations, both economical, logistical, and ethical, as well as the previous research done and knowledge already at hand on the ovine model led us to seek to provide a more exhaustive description of brain development during the last trimester of pregnancy in sheep by characterizing the cortical maturation of preterm lambs. This approach aimed to validate the relevance of this animal model for perinatal research. Cortical development was evaluated using immunohistochemical analysis of eight cellular and structural markers commonly impacted by prematurity in humans and other animal models: neurons, interneurons, synaptic vesicles, oligodendrocytes, myelin, astrocytes, and microglia (Mallard et al. 2014; Wallois et al. 2020).

2 | Materials and Methods

2.1 | Animals and Tissue Samples

Tissues were collected from time fixed pregnant ewes' fetuses, from "Ile-de-France" sheep lineage (RRID:NCBITaxon_9940). After 100 (n = 4) and 140 (n = 4) days of pregnancy (normal term = 145–150 days), caesarean sections were performed with a paralumbar approach after local anesthesia. Extremely preterm (n = 13) and late preterm (n = 13) fetal lambs were immediately euthanized after removal using Dolethal (pentobarbital, 10 mL, IM, Vetoquinol, Lure, France). Anatomical dissections were conducted within 1-h post-euthanasia. Brains were isolated and sampled, and separated into frontal lobe, parieto-temporal lobe, occipital lobe, and cerebellum. Half of the samples were immediately frozen in dry ice and stored at −80°C. The other half were placed in PFA 4% (paraformaldehyde 4%) and stored at 4°C for 3 days before their fixation in paraffin.

2.2 | Immunohistochemistry

2.2.1 | Antibodies

Neurons were studied by targeting NeuN (Millipore Cat# MAB377, RRID:AB_2298772), a neuron-specific protein expressed by most mature neurons during migration, as a marker for characterization (Mullen et al. 1992; Weyer and Schilling 2003). For interneurons, we targeted the expression of the calcium binding protein Calbindin-D28K (Swant Cat# cb38a, RRID:AB_3107026) that is mainly found in that cellular type (Floyd et al. 2018; Toledo-Rodriguez et al. 2004). Astrocytes were characterized using the Glial Fibrillary Acidic Protein (GFAP) (Agilent Cat# Z0334, RRID:AB_10013382), a sensitive and almost universal marker of astrocytes that increases in concentration at 28GW when astrocytes enter the intermediary area of the white matter (Poulot-Becq-Giraudon et al. 2022; Reske-Nielsen et al. 1987). To characterize microglia, we decided to target the ionized calcium-binding adaptor molecule 1 (Iba1) (FUJIFILM Wako Pure Chemical Corporation Cat# 019–19741, RRID:AB_839504), a microglial and macrophage specific calcium-binding protein.

TABLE 1 | Description of the antibodies, their targets, and their respective protocol for staining.

Antibody	Host	Target	Dilution	HIER	Counterstain	Supplier
Calbindin	Rabbit	Interneurons	1/10 000	ER2 10 min	5 min	Swant CB-38a
GFAP	Rabbit	Astrocytes	1/500	ER1 10 min	NA	Dako Z334
NeuN	Mouse	Neurons	1/1000	ER1 10 min	1 min	Merck MAB377
Olig2	Rabbit	Oligodendrocytes	1/200	ER2 20 min	1 min	IBL IBL18953
Synaptophysin	Mouse	Synaptic vesicles	1/100	ER1 10 min	5 min	Sigma S5768
MBP	Mouse	Myelin	1/1000	ER1 10 min	5 min	Merck MAB382
Iba1	Rabbit	Microglia	1/1000	ER1 10 min	5 min	Wako 019–19741

Note: ER1: pH 6.0 citrate buffer, ER2: pH 8.0 EDTA buffer.
Abbreviation: HIER: heat induced epitope retrieval.

Since oligodendrocytes originate from oligodendrocytes progenitor cells (OPCs) due to the influence of several transcription actors (Olig1, Olig2, Nkx2.2, and Sox10), we decided to target one of those transcription factors, namely Olig2 (IBL—America Cat# 18953, RRID:AB_2267671) known for oligodendrocytes differentiation, as our marker of choice. Regarding myelin, we decided to target one of its main components, the Myelin Basic Protein, or MBP (Millipore Cat# MAB382, RRID:AB_94971). As for synaptic vesicles, synaptophysin (Sigma-Aldrich Cat# S5768, RRID:AB_477523) is a protein found in virtually all neurons and neuroendocrine cells in the brain and interacting with synaptobrevin, an essential protein in synaptic vesicle, making it a perfect target for quantification and characterization (Calhoun et al. 1996; Wiedenmann et al. 1986).

2.2.2 | Antibody Characterization

The specificity and characterization of the antibodies used in this study are supported by multiple complementary sources. First, thanks to the manufacturer datasheets that provided validation data through immunoblotting and/or immunohistochemistry in commonly studied species such as mice, rats, and humans as well as other species in some cases (guinea pig, chicken, rabbit, or monkey) (Table 1). These data were further substantiated by peer-reviewed studies that have confirmed antibody specificity in various species and experimental contexts. For instance anti-synaptophysin in humans (Ip et al. 2011), mice (Frost et al. 2019), and rats (Bello-Medina et al. 2024); anti-Iba1 in mice (Deng et al. 2025) and rats (Fronczak et al. 2022); anti-Olig2 in mice (Isogai et al. 2015) and humans (Ohira et al. 2013); anti-calbindin 28k in mice (Boon et al. 2019); anti-NeuN in lamb (Fowke et al. 2018; Zhou et al. 2022); anti-MBP in mice (Chhor et al. 2017; Jarjour et al. 2008); and anti-GFAP in lamb (Joyeux et al. 2019; Mitchell et al. 2023). For each antibody, the observed staining patterns in our experiment were consistent with the one reported in previous studies.

2.2.3 | Immunohistochemistry

Immunostaining was performed on the UVSQ Histopathology platform Facility. Approximately 7 µm sections were prepared on the sagittal plane using Leica RM2265 microtome (Leica Biosystems RM2265 Fully Automated Rotary Microtome (RRID:SCR_018041) and placed on SuperFrost Plus slides (ref. J1800AMNZ) for each frontal, parieto-temporal and occipital lobe, and cerebellum. Immunohistochemistry was performed using an automated IHC stainer (Leica BOND-III Stainer RRID:SCR_026521). Sections were deparaffinized and rehydrated using Dewax Solution (AR9222) provided by Leica. Heat-induced epitope retrieval (HIER) varied according to the antibody supplier's suggestions and various on-site tests, using either pH 6.0 citrate buffer (ER1) or pH 8.0 EDTA buffer (ER2).

Primary antibodies were used at various concentrations based on the supplier's suggestions and adjustments (Table 1) and diluted using Bond Primary Antibody Diluent (AR9352). Primary antibodies were incubated during 60 min for each sample. Peroxydase-conjugated Donkey anti-mouse or anti-rabbit IgG secondary antibodies (Jackson ImmunoResearch Labs Cat# 715-035-151, RRID:AB_2340771 and Jackson ImmunoResearch Labs Cat# 711-036-152, RRID:AB_2340590, respectively) were used at a concentration of 1:200 for 30 min. Each slide was stained by immersion in mixed DAB for 5 min, while the time for counterstaining with hematoxylin varied according to the target and the antibody.

All staining reagents were part of the Bond Intense R Detection Kit (DS9263). After staining, sections were dehydrated through a series of baths: 70% ethanol, 90% ethanol, 100% ethanol for 3 min each, followed by a 5-min xylene bath. All slides were sealed and dry for a minimum of 24 h before image acquisition.

2.2.4 | Image Analysis

Pictures of each slide were collected using an AperioAT2 DX System (Leica Aperio AT2 DX System, RRID:SCR_027461) with a x20 objective and analyzed using QuPath (RRID:SCR_018257) (Bankhead et al. 2017). Image analysis was either performed on whole tissue or on selected area based on the type of staining (Figure 1).

For GFAP, MBP, Iba1, and calbindin, selections for whole tissue analysis were made using the Thresholder tool with a 32.26 µm/px resolution (extremely low) on Average Channel with a threshold of 230. Cleaning and correction of selection were performed manually. For each run, the stain vectors for hematoxylin and DAB were automatically estimated using the Estimate Stain

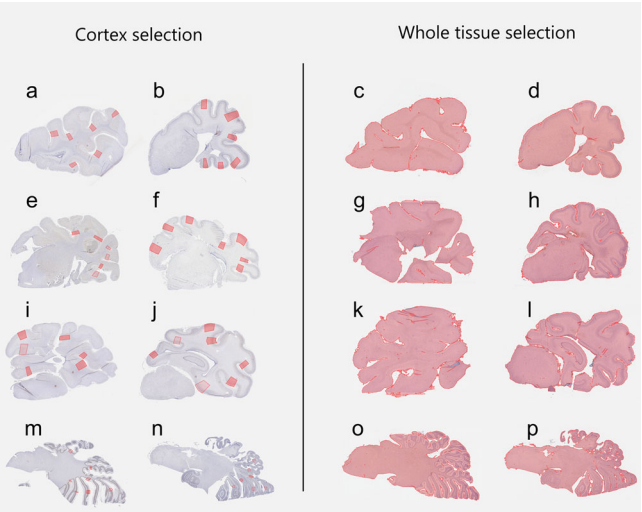

FIGURE 1 | Example in the cerebellum of manual selection of the cortex layers (left) and whole tissue selection (right) with 140 days lamb on the left side and 100 days on the right side for both selection examples. (a–d): frontal lobe; (e–h): parietal lobe; (i–l): occipital lobe; (m–p): cerebellum.

Vectors tool on the most representative slide, and new values were applied to each slide of the run. Quantification of signal intensity was done using positive pixel count with a 2.02 µm/px resolution (high) or 1.01 µm/px resolution (very high) targeting DAB with a threshold of 0.2 on the entire selection.

For NeuN and synaptophysin, 5–10 random areas encompassing all six cortical layers (from outside of the tissue to the white matter) were manually selected while Olig2 was analyzed by quantification of manually selected areas in the white matter. Stain vectors correction was applied for each run using the same method as previously. Quantification of cell density was performed through positive cell count using optical density sum with a 5 µm background radius, 1 µm median filter radius, 1.5 µM sigma, a 5 μm^2 minimum area and 0.2 µm single threshold for NeuN, and a 5 µm background radius, 2 µm median filter radius, 2 µm sigma, a 5 μm^2 minimum area and 0.2 µm single threshold for Olig2. Both settings used the Nucleus: DAB OD Mean as a score compartment to detect positive cells. Quantification of signal intensity for synaptophysin followed the same positive pixel count protocol as before.

Each comparison group included all 26 lambs with one image per marker per brain area per lamb. In case of folding of the tissues, problematic folds were removed by manual selecting the folds and excluding them from the analysis. Data normalization was performed by calculating the percentage of positivity per mm^2 of the analyzed surface. For positive cell counts requiring multiple manual selections, the mean percentage of positive cells per mm^2 across all selections per lamb was used

2.2.5 | Statistical Analysis

Statistical analyses were performed with R v4.4.3 (R Project for Statistical Computing, RRID:SCR_001905) in RStudio v2024.12.0+467 (RStudio, RRID:SCR_000432) using the tidyverse (tidyverse, RRID:SCR_019186), DescTools (DescTools, RRID:SCR_027454), coin (coin, RRID:SCR_027455), and rstatix packages (rstatix, RRID:SCR_021240) (Hothorn et al. 2006; Kassambara 2023; R Core Team 2024; Wickham et al. 2019). All samples are independent from each other and were treated as such. Extremely preterm fetal lambs (100 days) were compared to late preterm fetal lambs (140 days). Comparisons of proportions were performed with a Fisher test. Comparisons of means were performed using a Fisher–Pitman permutation test via the oneway_test function of the "coin" package version 1.4-3. Confidence intervals were calculated using a bootstrap approach with the MeanDiffCI function of the "DescTools" package version 0.99.60. *p*-values under 0.05 were considered statistically significant. Results are displayed as mean ± *SD* for the histological comparisons of the surface area of each section and mean difference [CI95] for the immunohistochemical analysis of each marker.

3 | Results

3.1 | Animal Comparison

The description of the two experimental groups is provided in Table 2. There was no difference in the number of lambs, as well as no statistically significant difference in the number of male and female fetal lambs (13 lambs [5 females and 8 males] in the extremely preterm group and 13 lambs [6 females and 7 males] in the late preterm group). However, there was a significant difference ($p < 0.001$) in the mean weight between the extremely preterm group (953 g [675; 1200]) and the late preterm group (3455 g [2370; 4875]).

The histological comparison revealed significant differences in the surface area of each section of the frontal lobe, parieto-temporal lobe, occipital lobe, and cerebellum between extremely preterm (100 days) and late preterm (140 days) fetal lambs, with sections from the late preterm group being significantly larger than the extremely preterm group. No significant difference was observed between male and female both within and between each group (data not shown). Due to these differences, the results from quantifications were normalized based on the surface area analyzed for each sample.

3.2 | Immunohistochemical Analysis

3.2.1 | Cellular Markers

The immunohistochemistry comparison of the number of positive neurons for NeuN (Figure 2a) between late preterm (140 days) and extremely preterm (100 days) showed no significant difference in the frontal lobe (5.49% [−1.4; 13.17], $p = 0.19$), the parietal lobe (7.44% [0.21; 15.15] $p = 0.06$), and the occipital lobe (5.67% [−1.46; 12.38] $p = 0.16$) when normalized by the area of analysis. However, the percentage of positivity was significantly higher in the cerebellum (26.51% [21.17; 31.64] $p < 0.001$) for lambs at late preterm compared to extremely preterm. When analyzing the granular layer of the cerebellum, we found that the mean cell area and mean percentage of NeuN-positive cells were both

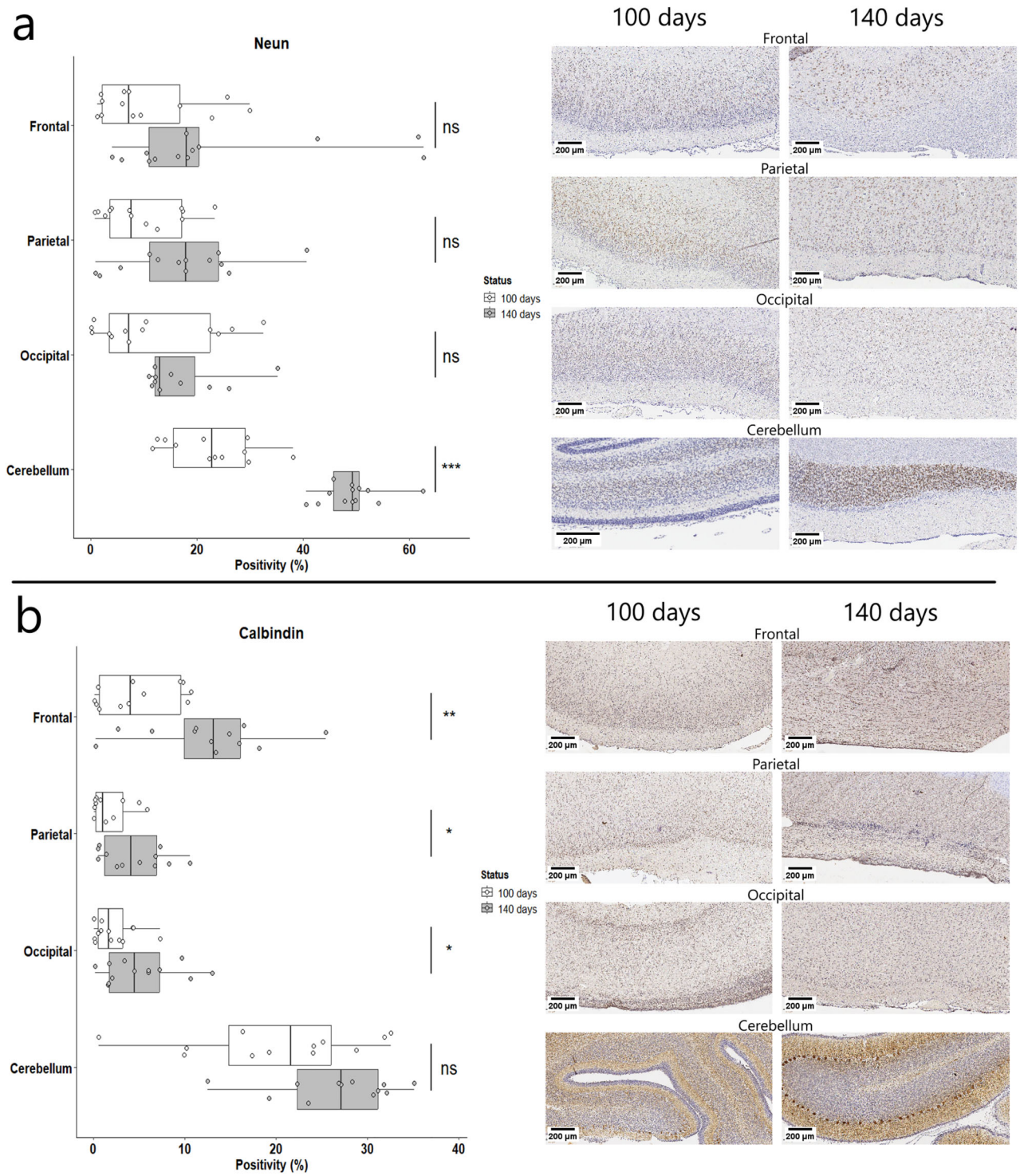

FIGURE 2 | Immunohistochemistry evaluation of positivity for NeuN (cortex) (a), and calbindin (whole tissue) (b) in the different brain areas at 100 days (white) and 140 days (grey), normalized by the surface of the analyzed area. n.s. = non-significant $p \geq 0.05$, $^{*}p < 0.05$, $^{**}p < 0.01$, $^{***}p < 0.001$.

significantly higher in the 140-days group compared to the 100 days-group (respectively, 4.12 mm^2 [0.87; 7.32] $p < 0.05$ (Figure 3a) and 53.78% [44.72; 60.96] $p < 0.0001$ (Figure 3b)). As analyzed zones were sampled at random over various areas of the cortex, these results can be generalized to the cerebellar cortex, reducing sampling bias and inter-lobules differences.

Conversely, the comparison of interneurons positive for calbindin (Figure 2b) showed significant differences between term and extremely preterm lambs regarding the frontal lobe, the parietal lobe and the occipital lobe (7.53% [3.1; 11.66] $p < 0.01$, 2.58% [0.3; 4.89] $p < 0.05$, and 3.05% [0.69; 5.38] $p < 0.05$) in 140-days fetal lamb, but no significant difference in the cerebellum (6.14% [−0.61; 12.69] $p = 0.07$).

TABLE 2 | Description of the experimental groups and statistical comparison of the mean surface area of each brain area between fetal sheep at 100 and 140 days.

Description	Extremely preterm (100 days)	Late preterm (140 days)	*p*-value
Animals			n.s.
Ewe	4	4	
Lambs	13	13	
Sex			n.s.
Female	5 (38%)	6 (46%)	
Male	8 (62%)	7 (54%)	
Weight in g (mean [min − max])	953 [675 − 1200]	3455 [2 370 − 4875]	***
Mean surface area in µm² (mean [min − max])			
Frontal lobe	153.76 [118.4 − 198.8]	244.65 [183.7 − 334]	***
Parietal lobe	252.16 [208.9 − 287.8]	433.53 [318.6 − 499]	****
Occipital lobe	195.32 [140.1 − 271.6]	271.7 [118 − 429.7]	*
Cerebellum	70.8 [31 − 136]	154.45 [104.4-239.8]	****

Abbreviation: n.s. = non-significant.
$p \geq 0.05$.
$^{*}p < 0.05$.
$^{***}p < 0.001$.
$^{****}p < 0.0001$.

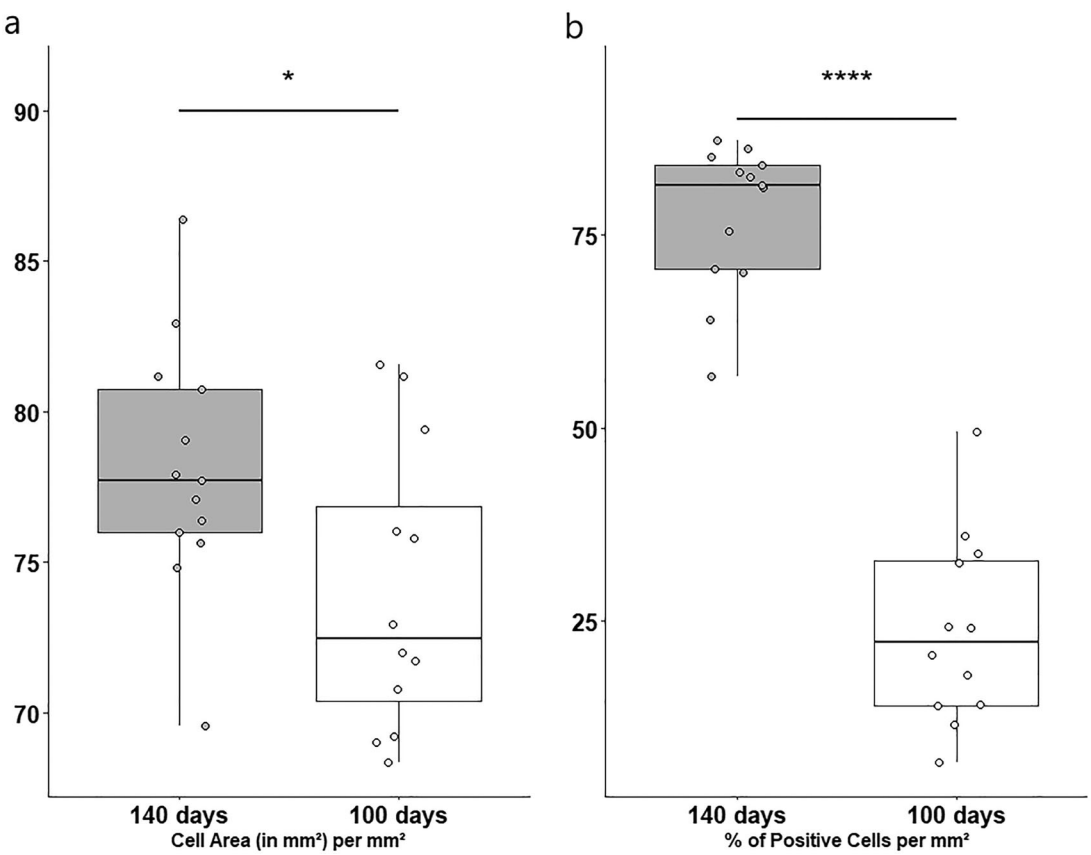

FIGURE 3 | Immunohistochemistry evaluation of the cell area in mm² (a), and percentage of NeuN-positive cells (b) in the granular layer of the cerebellum at 100 days (white) and 140 days (grey), normalized by the surface of the analyzed area. $^{*}p < 0.05$, $^{****}p < 0.0001$.

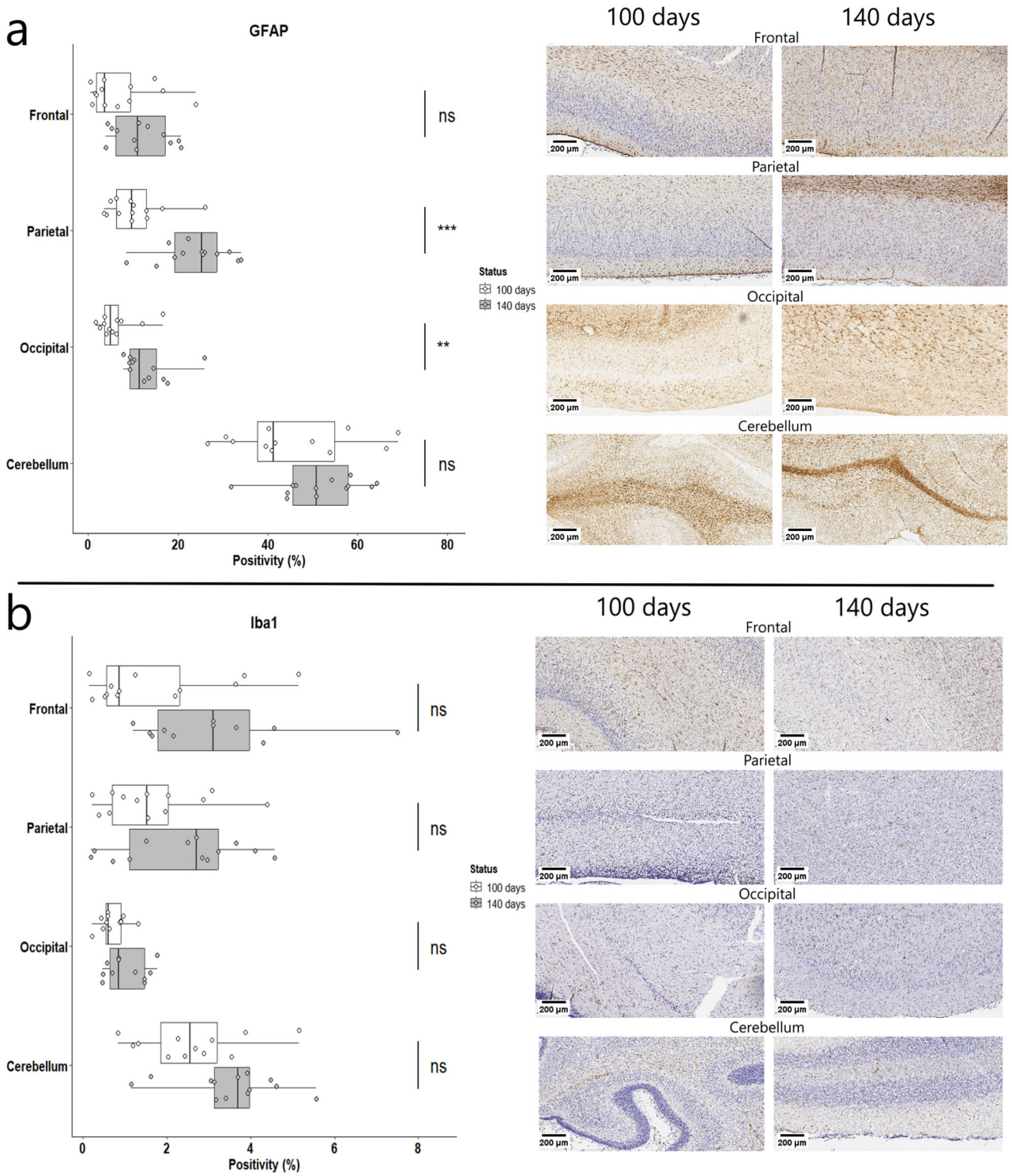

FIGURE 4 | Immunohistochemistry evaluation of positivity for GFAP (whole tissue) (a) and Iba1 (whole tissue) (b) in the different brain areas at 100 days (white) and 140 days (grey), normalized by the surface of the analyzed area. n.s. = non-significant $p \geq 0.05$, $^{*}p < 0.05$, $^{**}p < 0.01$, $^{***}p < 0.001$.

For astrocytes (Figure 4a**),** comparisons of GFAP staining between 100- and 140-days fetal lamb found no significant difference in the frontal lobe (4.4% [−0.98; 9.19] $p = 0.11$) and the cerebellum (5.75% [−3.89; 14.07], $p = 0.22$), but both the parietal lobe (13.46% [7.85; 17.8] $p < 0.001$) and the occipital lobe (7.8% [6.14; 11.48] $p < 0.01$) showed significantly higher mean positivity for the 140-days group.

Finally, Iba1 staining showed very low overall positivity with an average of 2%–4% positive cells in both groups. However, the consistency of the staining and positivity was such that we allowed ourselves to carry out a statistical comparison. No significant difference was found in any of the brain areas regarding Iba1 staining for microglia between 140- and 100-days lambs (Figure 4b) (respectively, 1.45% [0.21; 2.68] $p = 0.053$, 0.67% [−0.41; 1.57] $p = 0.2$, 0.34% [0.03; 0.69] $p = 0.056$ and 0.92% [0.01;

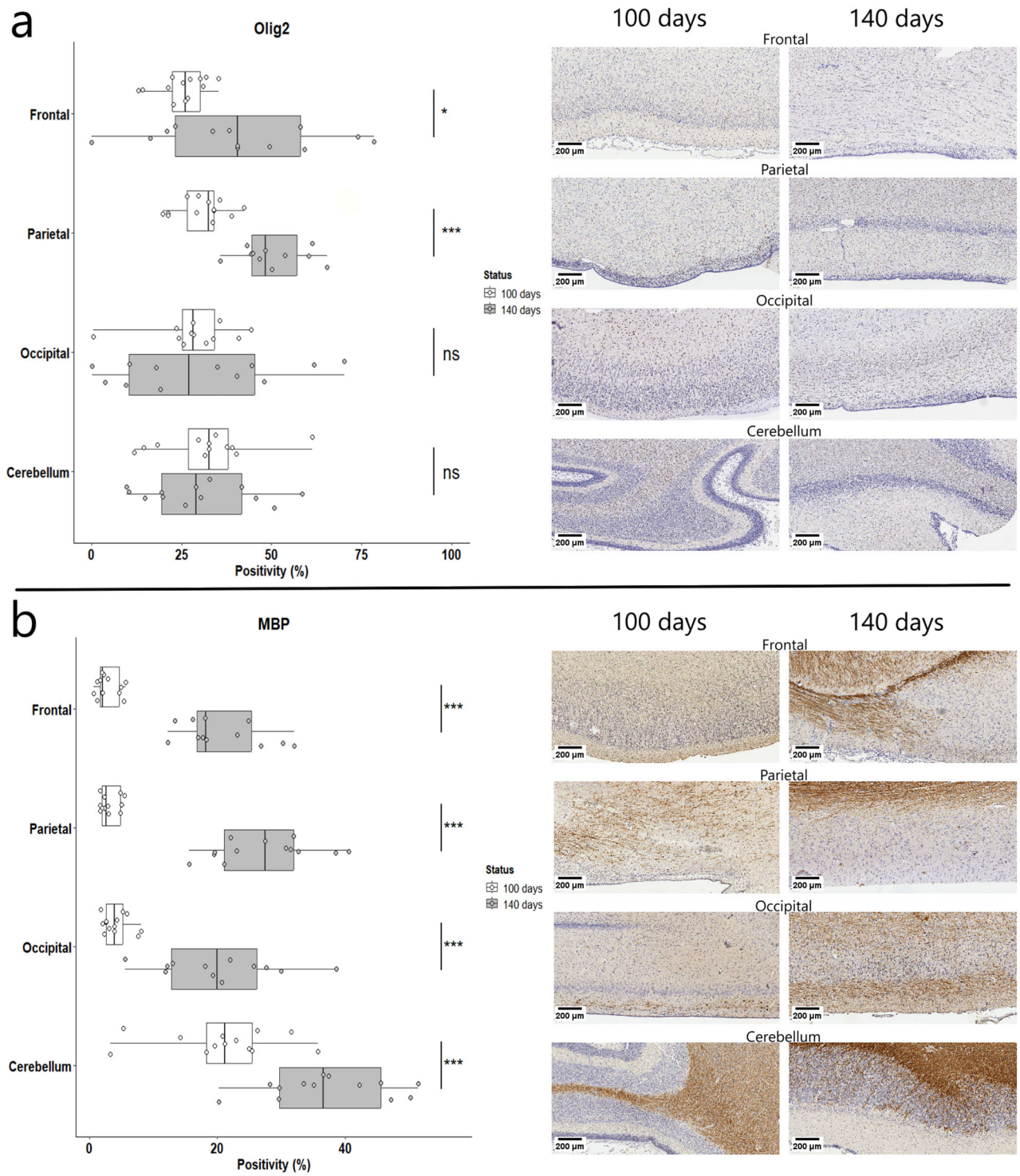

FIGURE 5 | Immunohistochemistry evaluation of positivity for Olig2 (white matter) (a) and MBP (whole tissue) (b) in the different brain areas at 100 days (white) and 140 days (grey), normalized by the surface of the analyzed area. n.s. = non-significant $p \geq 0.05$, $^{*}p < 0.05$, $^{**}p < 0.01$, $^{***}p < 0.001$.

1.76] $p = 0.072$ for frontal lobe, parietal lobe, occipital lobe, and cerebellum).

3.2.2 | Myelinization

Regarding the oligodendrocytes (Figure 5a), the percentage of positivity of Olig2 was significantly higher for 140-days fetal lambs in the frontal lobe (15.74% [3.12; 28.14] $p < 0.05$) and the parietal lobe (19.66% [13.86; 26.63] $p < 0.001$) with no significant difference between the two groups in the occipital lobe (1.36% [−12; 16.95] $p = 0.85$) and the cerebellum (−2.03% [12.47; 9.39] $p = 0.72$). However, immunohistochemistry analysis of MBP staining for the myelin sheath (Figure 5b) showed a significantly higher percentage of myelinization ($p < 0.001$) for 140-days fetal lambs in all four brain areas: frontal lobe (18.02% [14.38; 21.91]), parietal lobe (24.11%

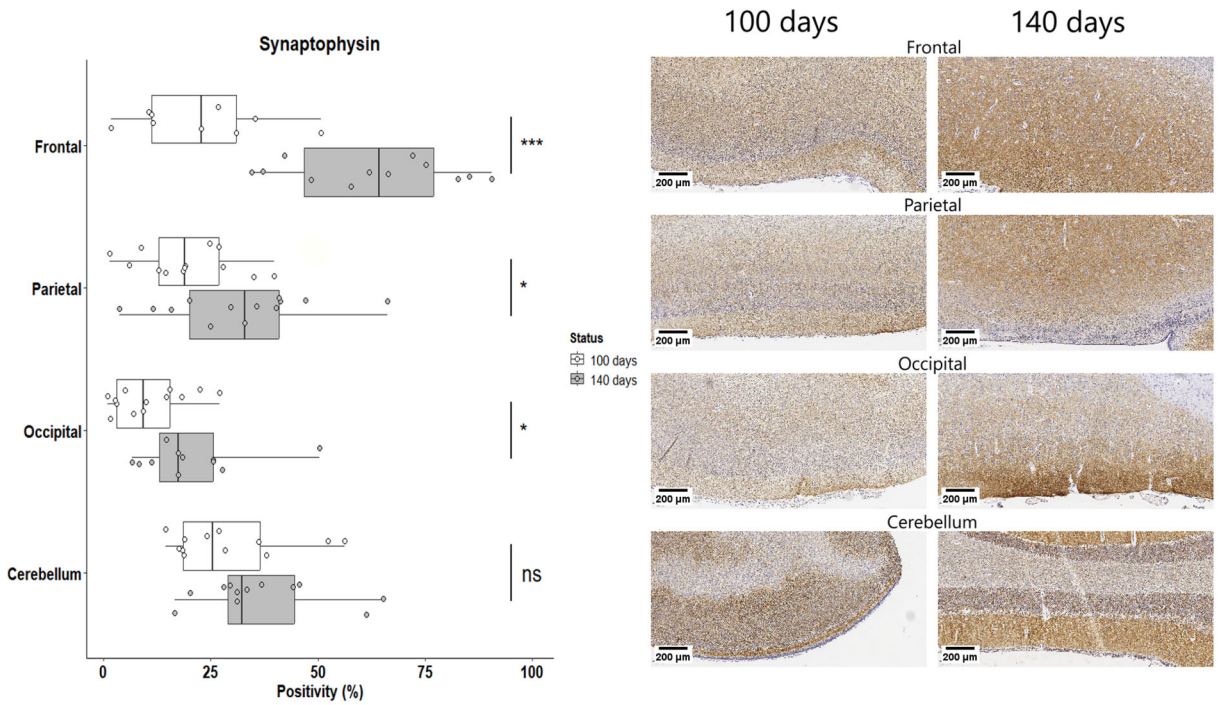

FIGURE 6 | Immunohistochemistry evaluation of positivity for synaptophysin (cortex) in the different brain areas at 100 days (white) and 140 days (grey), normalized by the surface of the analyzed area. n.s. = non-significant $p \geq 0.05$, $^{*}p < 0.05$, $^{**}p < 0.01$, $^{***}p < 0.001$.

[20.3; 28.18]), occipital lobe (16.29% [10.87; 21.98]), and cerebellum (16.71% [9.6; 23.99]) compared to 100-days fetal lambs.

3.2.3 | Synapses

The comparison of synaptic vesicle positive for synaptophysin (Figure 6) showed significant differences between late preterm and extremely preterm lambs regarding the frontal lobe, the parietal lobe and the occipital lobe (40.43% [25.57; 53.58] $p < 0.001$, 11.94% [2.92; 22.1] $p < 0.05$ and 9.73% [3.06; 19.89] $p < 0.05$) in 140-days fetal lamb, but no significant difference in the cerebellum (7.77% [2.37; 19.48] $p = 0.19$).

4 | Discussion

Preterm birth represents 10% of worldwide birth with about 5% being extremely preterm birth, with an increased risk of neurological impairment due to lower cortical surface and brain lesions, and a lower rate of survival. Current research offers an extensive understanding of the impact of extremely preterm birth on neurodevelopment in both humans and rodents. As the need for therapeutic alternatives for preterm care increases, recent studies (Cohen et al. 2024; Partridge et al. 2017) demonstrated that extra-uterine devices such as artificial placenta could allow for similar brain growth when used on extreme pre-term fetal lambs compared to same-age term fetal lambs who went through normal gestation. These studies showed promising data but highlight the need for a more exhaustive description of brain development in the lamb. Based on this premise, we aimed to provide detailed characterization and comparisons of the frontal lobe, the parieto-temporal lobe, the occipital lobe and the cerebellum during the last trimester of pregnancy in fetal lambs by targeting cellular and structural markers that are known to be impacted by prematurity. The specificity of the antibodies used during this study was assessed based on the low inter-species variability of these target antigens and the consistency of staining patterns observed in our experiments compared to those reported in the literature. Through immunohistochemical analyses, our results confirmed that extremely preterm birth is associated with significant alterations in brain maturation, both in terms of cortical surface and cellular and structural markers.

Noticeably, higher percentages of relative positivity were observed in 140-days term fetal lambs for calbindin and synaptophysin in the frontal, parietal, and occipital lobes. Calbindin-reactive interneurons are a subtype of GABAergic neurons playing a significant role in cortical development by providing excitatory drive (Aksenov et al. 2022; Letinic et al. 2002; Toledo-Rodriguez et al. 2004; Wang and Kriegstein 2009) while synaptophysin is a glycoprotein found in synaptic vesicles and playing a crucial role in neurotransmission (Ryan and Grant 2009). Those results indicate a more advanced development of GABA interneurons and higher synaptic activity in late preterm fetal lambs compared to extremely preterm fetal lambs, which corroborates with data in human and mouse showing a decrease in GABA signaling as well as synaptic dysfunction in extremely preterm infants (Stolp et al. 2019). However, there was no significant difference found in the proportion of NeuN-positive cells in the frontal, parietal and occipital lobe, unlike in the cerebellum where neurons were found in higher relative proportions in 140-days term fetal lambs. This lack of difference in most brain areas can be explained by the developmental kinetic of neurons, similar to that of humans where neuronal proliferation and migration in the cerebral cortex are mostly

TABLE 3 | Immunohistochemistry comparison of the percentage of NeuN-positive staining in each cortical layer and white matter for each brain region at 100 and 140 days, normalized by the surface of the analyzed area.

Brain areas	Cortical layers	Extreme preterm 100 days (mean [*SD*])	Extreme preterm 140 days (mean [*SD*])	Mean difference [IC 95%]	*p*-value.signif
Frontal lobe					
	Molecular layer	0.28 [0.27]	2.04 [1.39]	1.76 [0.74, 3.11]	ns
	External granular layer	0 [0]	12.98 [9.8]	12.98 [5.86, 23.03]	ns
	External pyramidal layer	0.05 [0.09]	25.51 [5.27]	25.46 [21.05, 29.88]	*
	Internal granular layer	0.4 [0.13]	25.58 [4.36]	25.18 [21.36, 28.95]	**
	Internal pyramidal layer	1.33 [1.95]	24.62 [11.46]	23.29 [14.68, 35.31]	*
	Multiform layer	1.81 [1.52]	20.99 [12.21]	19.18 [10.72, 31.79]	*
	White matter	0.39 [0.32]	0.58 [0.37]	0.19 [−0.14, 0.69]	ns
Parietal lobe					
	Molecular layer	0.23 [0.47]	0.93 [0.45]	0.7 [−0.04, 1.12]	ns
	External granular layer	0.34 [0.69]	4.01 [3.64]	3.67 [1.43, 7.74]	ns
	External pyramidal layer	0.09 [0.18]	18.51 [10.47]	18.42 [10.46, 27.2]	*
	Internal granular layer	5.3 [5.43]	26.2 [8.2]	20.9 [10.31, 27.15]	*
	Internal pyramidal layer	13.61 [2.38]	20.85 [8.03]	7.24 [0.43, 14.4]	ns
	Multiform layer	17.73 [2.94]	14.08 [9.95]	−3.65 [−12.91, 4.82]	ns
	White matter	5.39 [1.71]	0.71 [0.8]	−4.68 [−5.83, −2.68]	*
Occipital lobe					
	Molecular layer	1.78 [1.77]	3.6 [3]	1.82 [−0.87, 4.76]	ns
	External granular layer	2.72 [3.99]	8.53 [2.34]	5.81 [0.99, 9.02]	ns
	External pyramidal layer	7.36 [4.88]	17.3 [9.54]	9.94 [1.76, 19.42]	ns
	Internal granular layer	19.06 [5.94]	16.6 [8]	−2.46 [−12.13, 7.17]	ns
	Internal pyramidal layer	22.05 [8.5]	20.9 [9.57]	−1.15 [−12.88, 8.55]	ns
	Multiform layer	18.45 [9.66]	19.89 [4.43]	1.44 [−6.46, 11.49]	ns
	White matter	1.91 [1.2]	5.6 [3.12]	3.69 [1.44, 7.39]	ns
Cerebellum					
	Molecular layer	0 [0]	0.13 [0.26]	0.13 [0, 0.26]	ns
	External granular layer	0 [0]	0.27 [0.54]	0.27 [0, 0.54]	ns
	External pyramidal layer	7.41 [6.13]	13.89 [7.35]	6.48 [−2.25, 13.79]	ns
	Internal granular layer	30.96 [3.43]	79.22 [3.76]	48.26 [44.36, 53.8]	**
	Internal pyramidal layer	41.68 [15.32]	86.66 [2.21]	44.98 [31.64, 59.64]	*
	Multiform layer	35.52 [27.56]	83.97 [9.32]	48.45 [26.53, 76.93]	*
	White matter	0.49 [0.79]	1.15 [1.17]	0.66 −0.48, 1.91]	ns

Abbreviation: ns: non-significant.

*$p < 0.05$.

**$p < 0.01$.

done by 24 weeks of gestation, which is roughly equivalent to a 100 gestational days in lambs, with maturation going on up to 37 weeks of gestation (Adams-Chapman 2006). Regarding the difference in the cerebellum, it can be explained by the impact of extremely preterm birth on the cerebellar development (Barron and Kim 2020; Haldipur et al. 2011; Iskusnykh et al. 2018; Volpe 2009).

Similarly, significantly higher relative positivity was observed for Olig2, in the frontal and parietal lobe, and for MBP, in all four cerebral lobes of 140-days fetal lambs. Olig2 staining was used to assess oligodendrocytes, a type of glial cells involved in the structural plasticity of the brain (Monje 2018) and whose main function is the production of myelin, an extra membranous axonal structure primarily made of MBP and playing a major

TABLE 4 | Immunohistochemistry comparison of the percentage of calbindin-positive staining in each cortical layer and white matter for each brain region at 100 and 140 days, normalized by the surface of the analyzed area.

Brain areas	Cortical layers	Extreme preterm 100 days (mean [*SD*])	Extreme preterm 140 days (mean [*SD*])	Mean difference [IC 95%]	*p*-value.signif
Frontal lobe					
	Molecular layer	2.12 [2.11]	1.7 [0.33]	−0.42 [−2.55, 0.68]	ns
	External granular layer	4.38 [2.64]	1.85 [0.94]	−2.53 [−5.33, −0.53]	ns
	External pyramidal layer	4.15 [1.89]	1.21 [0.57]	−2.94 [−4.96, −1.69]	*
	Internal granular layer	2.9 [1.04]	1.11 [0.35]	−1.79 [−2.61, −0.85]	*
	Internal pyramidal layer	2.5 [0.97]	1.38 [0.27]	−1.12 [−1.86, −0.27]	ns
	Multiform layer	1.78 [0.9]	1.45 [0.61]	−0.33 [−1.12, 0.54]	ns
	White matter	1.63 [0.73]	2.14 [0.66]	0.51 [−0.32, 1.27]	ns
Parietal lobe					
	Molecular layer	2.74 [1.09]	1.84 [0.58]	−0.9 [−2.09, −0.12]	ns
	External granular layer	6.23 [3.88]	2.44 [1.11]	−3.79 [−7.23, −0.48]	ns
	External pyramidal layer	2.96 [1.94]	0.96 [0.35]	−2 [−3.55, −0.31]	ns
	Internal granular layer	1.33 [1.3]	1 [0.4]	−0.33 [−1.61, 0.77]	ns
	Internal pyramidal layer	1.7 [2.12]	1.23 [0.54]	−0.47 [−2.98, 0.93]	ns
	Multiform layer	1.6 [1.42]	1.69 [1.12]	0.09 [−1.37, 1.47]	ns
	White matter	1.24 [1.1]	3.51 [1.5]	2.27 [0.77, 3.92]	ns
Occipital lobe					
	Molecular layer	1.34 [0.46]	1.73 [1.49]	0.39 [−0.58, 2.05]	ns
	External granular layer	3.71 [2.44]	2.67 [1.27]	−1.04 [−3.06, 1.35]	ns
	External pyramidal layer	1.5 [1.26]	1.47 [0.67]	−0.03 [−1.28, 0.95]	ns
	Internal granular layer	0.6 [0.41]	1.16 [0.37]	0.56 [0.07, 0.94]	ns
	Internal pyramidal layer	0.47 [0.42]	1.06 [0.5]	0.59 [−0.02, 1.11]	ns
	Multiform layer	0.46 [0.35]	1.12 [0.44]	0.66 [0.26, 1.14]	ns
	White matter	0.35 [0.1]	1.13 [0.19]	0.78 [0.64, 1]	**
Cerebellum					
	Molecular layer	32.93 [17.55]	36.06 [22.41]	3.13 [−19.81, 29.84]	ns
	External granular layer	31.1 [17.3]	30.39 [25.39]	−0.71 [−20.08, 40.53]	ns
	External pyramidal layer	20.51 [12.43]	18.33 [17.7]	−2.18 [−17.13, 22.23]	ns
	Internal granular layer	6.11 [3.92]	6.08 [9.18]	−0.03 [−6.34, 11.13]	ns
	Internal pyramidal layer	6.49 [3.69]	5.56 [9.61]	−0.93 [−7.58, 11.5]	ns
	Multiform layer	21.77 [9.7]	6.64 [7.77]	−15.13 [−26.06, −5.78]	ns
	White matter	55.3 [12.81]	15.39 [9.76]	−39.91 [−52.96, −28.25]	*

Abbreviation: ns: non-significant.

*$p < 0.05$.

**$p < 0.01$.

role in maintaining the action potential while enabling faster propagation of the signal (Stadelmann et al. 2019). In humans, an increase in the number of oligodendrocytes is observed between 28 and 41 weeks of pregnancy, leading to a progressive increase in myelination, but were found to be disrupted in their progression in case of injury to the periventricular cerebral white matter at around 23–32 postconceptional weeks (Back 2017; Back et al. 2001, Back et al. 2006, Back et al. 2007; Jakovcevski and Zecevic 2005). Our results in lamb show a similar progression with a clear difference in the myelinization of the brain between late preterm and extremely preterm fetal lamb. This is further supported by the data collected (Partridge et al. 2017) showing

TABLE 5 | Immunohistochemistry comparison of the percentage of synaptophysin-positive staining in each cortical layer and white matter for each brain region at 100 and 140 days, normalized by the surface of the analyzed area.

Brain areas	Cortical layers	Extreme preterm 100 days (mean [*SD*])	Extreme preterm 140 days (mean [*SD*])	Mean difference [IC 95%]	*p*-value.signif
Frontal lobe					
	Molecular layer	5.65 [6.06]	80.33 [13.37]	74.68 [58.75, 83.81]	**
	External granular layer	0.54 [0.69]	84.79 [7.44]	84.25 [77.86, 90.42]	**
	External pyramidal layer	0.05 [0.05]	82.68 [4.78]	82.63 [77.62, 85.52]	**
	Internal granular layer	0.06 [0.02]	81.5 [5.09]	81.44 [77.22, 85.65]	**
	Internal pyramidal layer	0.04 [0.04]	79.49 [6.32]	79.45 [75.29, 86.02]	**
	Multiform layer	0.04 [0.05]	60.87 [7.11]	60.83 [56.62, 68.33]	**
	White matter	0.04 [0.03]	16.62 [19.4]	16.58 [6.05, 36.84]	ns
Parietal lobe					
	Molecular layer	29.1 [27.02]	18.31 [14.66]	−10.79 [−41.83, 11.13]	ns
	External granular layer	21.87 [19.67]	70.01 [24.49]	48.14 [20.64, 71.31]	*
	External pyramidal layer	3.89 [4.93]	51.23 [12.97]	47.34 [29.43, 55.73]	*
	Internal granular layer	4.48 [5.31]	58.62 [6.23]	54.14 [45.27, 60.24]	**
	Internal pyramidal layer	7.16 [7.07]	34.23 [6.11]	27.07 [18.35, 33.89]	*
	Multiform layer	3.74 [4]	4.95 [2.33]	1.21 [−3.9, 4.27]	ns
	White matter	1.49 [1.38]	0.09 [0.05]	−1.4 [−2.85, −0.48]	ns
Occipital lobe					
	Molecular layer	0.96 [1.03]	0.45 [0.71]	−0.51 [−1.52, 0.7]	ns
	External granular layer	0.81 [0.96]	0.28 [0.46]	−0.53 [−1.55, 0.22]	ns
	External pyramidal layer	0.02 [0.01]	0.41 [0.46]	0.39 [0.09, 0.88]	ns
	Internal granular layer	0.13 [0.17]	0.15 [0.24]	0.02 [−0.2, 0.35]	ns
	Internal pyramidal layer	0.14 [0.17]	0.04 [0.04]	−0.1 [−0.26, 0.03]	ns
	Multiform layer	0.19 [0.24]	0.03 [0.06]	−0.16 [−0.45, 0]	ns
	White matter	0.04 [0.04]	0.05 [0.09]	0.01 [−0.05, 0.12]	ns
Cerebellum					
	Molecular layer	33 [23.28]	91.89 [3.31]	58.89 [42.09, 77.84]	**
	External granular layer	18.46 [15.68]	43.82 [13.21]	25.36 [9.18, 41.21]	*
	External pyramidal layer	10.92 [11.81]	43.99 [10.6]	33.07 [20.91, 46.09]	*
	Internal granular layer	16.51 [10.67]	38.75 [8.43]	22.24 [12.08, 32.97]	*
	Internal pyramidal layer	14.76 [7.31]	41.89 [10.77]	27.13 [17.12, 38.04]	*
	Multiform layer	8.37 [7]	13.27 [9.83]	4.9 [−3.8, 16.16]	ns
	White matter	1.43 [2.22]	5.57 [6.85]	4.14 [−0.88, 10.21]	ns

Abbreviation: ns: non-significant.
*$p < 0.05$.
**$p < 0.01$.

a regular myelinization kinetics in extremely preterm lamb on extra-uterine support.

Likewise, we characterized astrocytes and microglia, two subtypes of glial cells with numerous functions, ranging from homeostasis regulation to defining cortical architecture for astrocytes (Verkhratsky and Nedergaard 2018), and controlling neuronal differentiation, playing a role in synaptic pruning and immune response as well as several other roles for microglia (Hattori 2023; Hickman et al. 2018; Ikegami et al. 2019; Santos et al. 2020). We described those two cellular types using respectively GFAP and Iba1 as markers and found a significantly higher relative proportion of astrocytes in the parietal and occipital lobe of term fetal lambs, with a general trend in higher relative proportion overall. Since GFAP staining was analyzed on whole tissue selection, with normalization on based on the analyzed selection, this difference

between the two groups can be explained by the difference in brain maturation. While astrocytes are found in every area of the brain at 17GW in humans, that observed difference is similar to what can be seen in normal human fetal brain where astrocytes increase in size and number at 22GW (Reske-Nielsen et al. 1987). However, no significant difference was found for microglia in any of the analyzed brain area. This is similar to what can be found in the human brain as microglial entry and colonization as well as overall microglial development happens the earliest in brain development, with peak density happening at roughly 24 weeks of gestation (Menassa and Gomez-Nicola 2018).

Overall, our findings align with the known neurodevelopmental alterations and impact of extremely preterm birth reported in humans and other animal models, supporting the validity of the lambs as a pre-clinical model in studying pathologies and therapeutic alternatives for extremely preterm birth. As such, our data greatly contribute to the current scientific literature dedicated to the sheep as a model for pregnancies and developmental biology by deepening our understanding of brain development in that model.

However, the relatively small size of our groups may hamper the detection of smaller differences between our two groups. In addition, our study focused on large brain areas and markers, and the lack of molecular analyses such as transcriptomic does not allow us to have a more precise analysis of the difference between extremely preterm and late preterm fetal lambs in terms of gene expression for each marker nor is it possible to assess other phenomenon such as inflammation. The use of relatively broad markers such as Olig2, which does not differentiate between different type of cells within the lineage of oligodendrocytes, or calbindin, which also stains Purkinje cells that are unique to the cerebellum in addition to staining interneurons, means that further studies using more specifics markers would be necessary to obtain a finer characterization.

Furthermore, our study did not include inter-areal or inter-zonal comparison of staining within each sample but rather focused on the overall quantification of markers. That decision was made due to the high variability of the delineation of cortical layers, which would introduce the substantial risk of selection bias, and supported by a small-scale analysis of NeuN, calbindin, and synaptophysin (Tables 3–5). However, that decision can induce a bias in the interpretation of the data as positivity of staining can vary depending on the analyzed area of the brain. Similarly, more comprehensive and accurate findings could have been obtained through tissue clearing or stereological analysis of our samples.

Finally, as the extremely preterm birth in our study was non-pathologically induced, our data might not reflect the actual of the events taking place during a naturally occurring extremely preterm birth, namely the activation of microglia, cell death or brain injuries resulting from hypoxia or inflammation. Future studies should explore more diverse brain areas with a larger sample size, additional markers and finer analyses, such as single cell in situ profiling, in order to draw a more accurate description of the cortical development in lambs, its alterations by pathologies and its differences or similarities with human development.

5 | Conclusion

In conclusion, our study provides a comprehensive description of cortical maturation between extremely preterm and late preterm fetal lambs and highlights the similarities with human development, particularly an antero–posterior development regarding a selection of cellular and structural markers. These results support the use of fetal lamb as an animal model for extremely preterm birth and pathologies that alter brain development.

Author Contributions

E.M.S. and F.V. conceptualized the study. Animal procedures were performed by V.M., E.M.S., L.C., F.C., M.D., P.B., A.T., O.S., and F.V. Histological analyses were performed by YR with some regular help from L.C., O.L.C., P.G., and L.S. Y.R. collected data, performed statistical analysis and drafted the initial manuscript. E.M.S., V.M., and F.V. reviewed the manuscript for important intellectual content. All authors revised the manuscript and approved the final manuscript as submitted and agreed to be accountable for all aspects of the work.

Acknowledgment

The authors greatly acknowledge the UVSQ Histopathology platform Facility.

Open access publication funding provided by COUPERIN CY26.

Funding

This research received funding from the Institut de Recherche en Santé de la Femme (IRSF).

Ethics Statement

All procedures carried out in the present study were approved by the French Ethical Committee n°16 under protocol APAFIS#22584–2019102411142765.

Conflicts of Interest

The authors declare no conflicts of interest.

Data Availability Statement

The data that support the findings of this study are available from the corresponding author upon reasonable request.

Peer Review

For transparency, the peer review documents associated with this article are available at https://doi.org/10.1002/cne.70149.

References

Adams-Chapman, I. 2006. "Neurodevelopmental Outcome of the Late Preterm Infant." *Clinics in Perinatology* 33, no. 4: 947–964. https://doi.org/10.1016/j.clp.2006.09.004.

Adams-Chapman, I., R. J. Heyne, S. B. DeMauro, et al. 2018. "Neurodevelopmental Impairment Among Extremely Preterm Infants in the Neonatal Research Network." *Pediatrics* 141, no. 5: e20173091. https://doi.org/10.1542/peds.2017-3091.

Ajayi-Obe, M., N. Saeed, F. M. Cowan, M. A. Rutherford, and A. D. Edwards. 2000. "Reduced Development of Cerebral Cortex in Extremely

Preterm Infants." *Lancet* 356, no. 9236: 1162–1163. https://doi.org/10.1016/s0140-6736(00)02761-6.

Aksenov, D. P., D. A. Gascoigne, J. Duan, and A. Drobyshevsky. 2022. "Function and Development of Interneurons Involved in Brain Tissue Oxygen Regulation." *Frontiers in Molecular Neuroscience* 15: 1069496. https://doi.org/10.3389/fnmol.2022.1069496.

Back, S. A. 2017. "White Matter Injury in the Preterm Infant: Pathology and Mechanisms." *Acta Neuropathologica* 134, no. 3: 331–349. https://doi.org/10.1007/s00401-017-1718-6.

Back, S. A., N. L. Luo, N. S. Borenstein, J. M. Levine, J. J. Volpe, and H. C. Kinney. 2001. "Late Oligodendrocyte Progenitors Coincide With the Developmental Window of Vulnerability for Human Perinatal White Matter Injury." *Journal of Neuroscience* 21, no. 4: 1302–1312. https://doi.org/10.1523/JNEUROSCI.21-04-01302.2001.

Back, S. A., A. Riddle, and A. R. Hohimer. 2006. "Role of Instrumented Fetal Sheep Preparations in Defining the Pathogenesis of Human Periventricular White-Matter Injury." *Journal of Child Neurology* 21, no. 7: 582–589. https://doi.org/10.1177/08830738060210070101.

Back, S. A., A. Riddle, and M. M. McClure. 2007. "Maturation-Dependent Vulnerability of Perinatal White Matter in Premature Birth." *Supplement, Stroke* 38, no. S2: 724–730. https://doi.org/10.1161/01.STR.0000254729.27386.05.

Bankhead, P., M. B. Loughrey, J. A. Fernández, et al. 2017. "QuPath: Open Source Software for Digital Pathology Image Analysis." *Scientific Reports* 7, no. 1: 1. https://doi.org/10.1038/s41598-017-17204-5.

Banstola, A., and J. N. J. Reynolds. 2022. "The Sheep as a Large Animal Model for the Investigation and Treatment of Human Disorders." *Biology* 11, no. 9: 1251. https://doi.org/10.3390/biology11091251.

Barron, T., and J. H. Kim. 2020. "Preterm Birth Impedes Structural and Functional Development of Cerebellar Purkinje Cells in the Developing Baboon Cerebellum." *Brain Sciences* 10, no. 12: 897. https://doi.org/10.3390/brainsci10120897.

Barry, J. S., and R. V. Anthony. 2008. "The Pregnant Sheep as a Model for Human Pregnancy." *Theriogenology* 69, no. 1: 55–67. https://doi.org/10.1016/j.theriogenology.2007.09.021.

Bello-Medina, P. C., M. Díaz-Muñoz, S. T. Martín del Campo, et al. 2024. "A Maternal Low-Protein Diet Results in Sex-Specific Differences in Synaptophysin Expression and Milk Fatty Acid Profiles in Neonatal Rats." *Journal of Nutritional Science* 13: e64. https://doi.org/10.1017/jns.2024.46.

Blencowe, H., S. Cousens, M. Z. Oestergaard, et al. 2012. "National, Regional, and Worldwide Estimates of Preterm Birth Rates in the Year 2010 With Time Trends Since 1990 for Selected Countries: A Systematic Analysis and Implications." *Lancet* 379, no. 9832: 2162–2172. https://doi.org/10.1016/S0140-6736(12)60820-4.

Boon, J., E. Clarke, N. Kessaris, A. Goffinet, Z. Molnár, and A. Hoerder-Suabedissen. 2019. "Long-Range Projections From Sparse Populations of GABAergic Neurons in Murine Subplate." *Journal of Comparative Neurology* 527, no. 10: 1610–1620. https://doi.org/10.1002/cne.24592.

Calhoun, M. E., M. Jucker, L. J. Martin, G. Thinakaran, D. L. Price, and P. R. Mouton. 1996. "Comparative Evaluation of Synaptophysin-Based Methods for Quantification of Synapses." *Journal of Neurocytology* 25, no. 1: 821–828. https://doi.org/10.1007/BF02284844.

Chhor, V., R. Moretti, T. Le Charpentier, et al. 2017. "Role of Microglia in a Mouse Model of Paediatric Traumatic Brain Injury." *Brain, Behavior, and Immunity* 63: 197–209. https://doi.org/10.1016/j.bbi.2016.11.001.

Cohen, J. L., F. De Bie, A. N. Viaene, et al. 2024. "Extrauterine Support of Pre-Term Lambs Achieves Similar Transcriptomic Profiling to Late Pre-Term Lamb Brains." *Scientific Reports* 14, no. 1: 28840. https://doi.org/10.1038/s41598-024-79095-7.

Deng, S., Z. Zhang, L. Liu, et al. 2025. "The E3 Ligase c-Cbl Modulates Microglial Phenotypes and Contributes to Parkinson's Disease Pathology." *Cell Death Discovery* 11: 184. https://doi.org/10.1038/s41420-025-02482-0.

Floyd, T. L., Y. Dai, and D. R. Ladle. 2018. "Characterization of Calbindin D28k Expressing Interneurons in the Ventral Horn of the Mouse Spinal Cord." *Developmental Dynamics* 247, no. 1: 185–193. https://doi.org/10.1002/dvdy.24601.

Fowke, T. M., R. Galinsky, J. O. Davidson, et al. 2018. "Loss of Interneurons and Disruption of Perineuronal Nets in the Cerebral Cortex Following Hypoxia-Ischaemia in Near-Term Fetal Sheep." *Scientific Reports* 8, no. 1: 17686. https://doi.org/10.1038/s41598-018-36083-y.

Fronczak, K. M., A. Roberts, S. Svirsky, et al. 2022. "Assessment of Behavioral, Neuroinflammatory, and Histological Responses in a Model of Rat Repetitive Mild Fluid Percussion Injury at 2 Weeks Post-Injury." *Frontiers in Neurology* 13: 945735. https://doi.org/10.3389/fneur.2022.945735.

Frost, P. S., F. Barros-Aragão, R. T. da Silva, et al. 2019. "Neonatal Infection Leads to Increased Susceptibility to Aβ Oligomer-Induced Brain Inflammation, Synapse Loss and Cognitive Impairment in Mice." *Cell Death & Disease* 10, no. 4: 323. https://doi.org/10.1038/s41419-019-1529-x.

Haldipur, P., U. Bharti, C. Alberti, et al. 2011. "Preterm Delivery Disrupts the Developmental Program of the Cerebellum." *PLoS ONE* 6, no. 8: e23449. https://doi.org/10.1371/journal.pone.0023449.

Hattori, Y. 2023. "The Multifaceted Roles of Embryonic Microglia in the Developing Brain." *Frontiers in Cellular Neuroscience* 17: 988952. https://www.frontiersin.org/articles/10.3389/fncel.2023.988952.

Hickman, S., S. Izzy, P. Sen, L. Morsett, and J. E. Khoury. 2018. "Microglia in Neurodegeneration." *Nature Neuroscience* 21, no. 10: 1359–1369. https://doi.org/10.1038/s41593-018-0242-x.

Hothorn, T., K. Hornik, M. A. van de Wiel, and A. Zeileis. 2006. "A Lego System for Conditional Inference." *American Statistician* 60, no. 3: 257–263. https://doi.org/10.1198/000313006×118430.

Ikegami, A., K. Haruwaka, and H. Wake. 2019. "Microglia: Lifelong Modulator of Neural Circuits." *Neuropathology* 39, no. 3: 173–180. https://doi.org/10.1111/neup.12560.

Inder, T. E., S. K. Warfield, H. Wang, P. S. Hüppi, and J. J. Volpe. 2005. "Abnormal Cerebral Structure Is Present at Term in Premature Infants." *Pediatrics* 115, no. 2: 286–294. https://doi.org/10.1542/peds.2004-0326.

Ip, B. K., N. Bayatti, N. J. Howard, S. Lindsay, and G. J. Clowry. 2011. "The Corticofugal Neuron-Associated Genes ROBO1, SRGAP1, and CTIP2 Exhibit an Anterior to Posterior Gradient of Expression in Early Fetal Human Neocortex Development." *Cerebral Cortex* 21, no. 6: 1395–1407. https://doi.org/10.1093/cercor/bhq219.

Iskusnykh, I. Y., R. K. Buddington, and V. V. Chizhikov. 2018. "Preterm Birth Disrupts Cerebellar Development by Affecting Granule Cell Proliferation Program and Bergmann Glia." *Experimental Neurology* 306: 209–221. https://doi.org/10.1016/j.expneurol.2018.05.015.

Isogai, E., K. Okumura, M. Saito, et al. 2015. "Oncogenic Lmo3 Cooperates With Hen2 to Induce Hydrocephalus in Mice." *Experimental Animals* 64, no. 4: 407–414. https://doi.org/10.1538/expanim.15-0026.

Jakovcevski, I., and N. Zecevic. 2005. "Sequence of Oligodendrocyte Development in the Human Fetal Telencephalon." *Glia* 49, no. 4: 480–491. https://doi.org/10.1002/glia.20134.

Jarjour, A. A., S.-J. Bull, M. Almasieh, et al. 2008. "Maintenance of Axo-Oligodendroglial Paranodal Junctions Requires DCC and Netrin-1." *Journal of Neuroscience* 28, no. 43: 11003–11014. https://doi.org/10.1523/JNEUROSCI.3285-08.2008.

Joyeux, L., A. C. Engels, J. Van Der Merwe, et al. 2019. "Validation of the Fetal Lamb Model of Spina Bifida." *Scientific Reports* 9, no. 1: 9327. https://doi.org/10.1038/s41598-019-45819-3.

Kassambara, A. 2023. "rstatix: Pipe-Friendly Framework for Basic Statistical Tests (Version 0.7.2) [Logiciel]." https://cran.r-project.org/web/packages/rstatix/index.html.

Letinic, K., R. Zoncu, and P. Rakic. 2002. "Origin of GABAergic Neurons in the Human Neocortex." *Nature* 417, no. 6889: 645–649. https://doi.org/10.1038/nature00779.

Mallard, C., J. O. Davidson, S. Tan, et al. 2014. "Astrocytes and Microglia in Acute Cerebral Injury Underlying Cerebral Palsy Associated With Preterm Birth." *Pediatric Research* 75, no. 1: 1. https://doi.org/10.1038/pr.2013.188.

Menassa, D. A., and D. Gomez-Nicola. 2018. "Microglial Dynamics During Human Brain Development." *Frontiers in Immunology* 9: 01014. https://www.frontiersin.org/articles/10.3389/fimmu.2018.01014.

Mitchell, N. L., S. J. Murray, M. P. Wellby, et al. 2023. "Long-Term Safety and Dose Escalation of Intracerebroventricular CLN5 Gene Therapy in Sheep Supports Clinical Translation for CLN5 Batten Disease." *Frontiers in Genetics* 14: 1212228. https://doi.org/10.3389/fgene.2023.1212228.

Monje, M. 2018. "Myelin Plasticity and Nervous System Function." *Annual Review of Neuroscience* 41: 61–76. https://doi.org/10.1146/annurev-neuro-080317-061853.

Morin, C., D. Guenoun, I. Sautet, et al. 2022. "The Impact of Mouse Preterm Birth Induction by RU-486 on Microglial Activation and Subsequent Hypomyelination." *International Journal of Molecular Sciences* 23, no. 9: 4867. https://doi.org/10.3390/ijms23094867.

Mullen, R. J., C. R. Buck, and A. M. Smith. 1992. "NeuN, a Neuronal Specific Nuclear Protein in Vertebrates." *Development* 116, no. 1: 201–211. https://doi.org/10.1242/dev.116.1.201.

Ohira, K., R. Takeuchi, H. Shoji, and T. Miyakawa. 2013. "Fluoxetine-Induced Cortical Adult Neurogenesis." *Neuropsychopharmacology* 38, no. 6: 909–920. https://doi.org/10.1038/npp.2013.2.

Partridge, E. A., M. G. Davey, M. A. Hornick, et al. 2017. "An Extra-Uterine System to Physiologically Support the Extreme Premature Lamb." *Nature Communications* 8, no. 1: 1. https://doi.org/10.1038/ncomms15112.

Peterson, B. S., B. Vohr, L. H. Staib, et al. 2000. "Regional Brain Volume Abnormalities and Long-Term Cognitive Outcome in Preterm Infants." *JAMA* 284, no. 15: 1939–1947. https://doi.org/10.1001/jama.284.15.1939.

Pierrat, V., L. Marchand-Martin, S. Marret, et al. 2021. "Neurodevelopmental Outcomes at Age 5 Among Children Born Preterm: EPIPAGE-2 Cohort Study." *BMJ* 373: n741. https://doi.org/10.1136/bmj.n741.

Poulot-Becq-Giraudon, Y., M.-A. C. Sauvage, and C. Escartin. 2022. "Astrocytes Réactifs et Maladies Cérébrales—Biomarqueurs et Cibles Thérapeutiques." *Médecine/Sciences* 38, no. 10: 10. https://doi.org/10.1051/medsci/2022104.

R Core Team. 2024. *R: A Language and Environment for Statistical Computing*. R Foundation for Statistical Computing.

Reske-Nielsen, E., S. Oster, and I. Reintoft. 1987. "Astrocytes in the Prenatal Central Nervous System." *Acta Pathologica Microbiologica Scandinavica Series A: Pathology* 95A, no. 1-6: 339–346. https://doi.org/10.1111/j.1699-0463.1987.tb00050_95A.x.

Ryan, T. J., and S. G. N. Grant. 2009. "The Origin and Evolution of Synapses." *Nature Reviews Neuroscience* 10, no. 10: 10. https://doi.org/10.1038/nrn2717.

Santos, S. E. D., M. Medeiros, J. Porfirio, et al. 2020. "Similar Microglial Cell Densities Across Brain Structures and Mammalian Species: Implications for Brain Tissue Function." *Journal of Neuroscience* 40, no. 24: 4622. https://doi.org/10.1523/JNEUROSCI.2339-19.2020.

Stadelmann, C., S. Timmler, A. Barrantes-Freer, and M. Simons. 2019. "Myelin in the Central Nervous System: Structure, Function, and Pathology." *Physiological Reviews* 99, no. 3: 1381–1431. https://doi.org/10.1152/physrev.00031.2018.

Stolp, H. B., B. Fleiss, Y. Arai, et al. 2019. "Interneuron Development Is Disrupted in Preterm Brains With Diffuse White Matter Injury: Observations in Mouse and Human." *Frontiers in Physiology* 10: 955. https://doi.org/10.3389/fphys.2019.00955.

Toledo-Rodriguez, M., B. Blumenfeld, C. Wu, et al. 2004. "Correlation Maps Allow Neuronal Electrical Properties to be Predicted From Single-Cell Gene Expression Profiles in Rat Neocortex." *Cerebral Cortex* 14, no. 12: 1310–1327. https://doi.org/10.1093/cercor/bhh092.

Tomassoni, D., L. Di Cesare Mannelli, V. Bramanti, C. Ghelardini, F. Amenta, and A. Pacini. 2018. "Treatment With Acetyl-L-Carnitine Exerts a Neuroprotective Effect in the Sciatic Nerve Following Loose Ligation: A Functional and Microanatomical Study." *Neural Regeneration Research* 13, no. 4: 692. https://doi.org/10.4103/1673-5374.230297.

Torchin, H., P.-Y. Ancel, P.-H. Jarreau, and F. Goffinet. 2015. "Épidémiologie de la Prématurité: Prévalence, Évolution, Devenir Des Enfants." *Journal de Gynécologie Obstétrique et Biologie de la Reproduction* 44, no. 8: 723–731. https://doi.org/10.1016/j.jgyn.2015.06.010.

Verkhratsky, A., and M. Nedergaard. 2018. "Physiology of Astroglia." *Physiological Reviews* 98, no. 1: 239–389. https://doi.org/10.1152/physrev.00042.2016.

Volpe, J. J. 2005. "Encephalopathy of Prematurity Includes Neuronal Abnormalities." *Pediatrics* 116, no. 1: 221–225. https://doi.org/10.1542/peds.2005-0191.

Volpe, J. J. 2009. "Cerebellum of the Premature Infant: Rapidly Developing, Vulnerable, Clinically Important." *Journal of Child Neurology* 24, no. 9: 1085–1104. https://doi.org/10.1177/0883073809338067.

Walani, S. R. 2020. "Global Burden of Preterm Birth." *International Journal of Gynaecology and Obstetrics* 150, no. 1: 31–33. https://doi.org/10.1002/ijgo.13195.

Wallois, F., L. Routier, and E. Bourel-Ponchel. 2020. "Impact of Prematurity on Neurodevelopment." In *Handbook of Clinical Neurology*, edited by A. Gallagher C. Bulteau D. Cohen, and J. L. Michaud, 341–375. Elsevier. https://doi.org/10.1016/B978-0-444-64150-2.00026-5.

Wang, D. D., and A. R. Kriegstein. 2009. "Defining the Role of GABA in Cortical Development." *Journal of Physiology* 587, no. Pt 9: 1873–1879. https://doi.org/10.1113/jphysiol.2008.167635.

Weyer, A., and K. Schilling. 2003. "Developmental and Cell Type-Specific Expression of the Neuronal Marker NeuN in the Murine Cerebellum." *Journal of Neuroscience Research* 73, no. 3: 400–409. https://doi.org/10.1002/jnr.10655.

WHO. 2023. "Born Too Soon: Decade of Action on Preterm Birth." https://www.who.int/publications/i/item/9789240073890.

Wickham, H., M. Averick, J. Bryan, et al. 2019. "Welcome to the Tidyverse." *Journal of Open Source Software* 4, no. 43: 1686. https://doi.org/10.21105/joss.01686.

Wiedenmann, B., W. W. Franke, C. Kuhn, R. Moll, and V. E. Gould. 1986. "Synaptophysin: A Marker Protein for Neuroendocrine Cells and Neoplasms." *Proceedings of the National Academy of Sciences of the United States of America* 83, no. 10: 3500–3504.

Yuan, A., M. V. Rao, n. Veeranna, and R. A. Nixon. 2012. "Neurofilaments at a Glance." *Journal of Cell Science* 125, no. Pt 14: 3257–3263. https://doi.org/10.1242/jcs.104729.

Zhou, K. Q., L. Bennet, G. Wassink, et al. 2022. "Persistent Cortical and White Matter Inflammation After Therapeutic Hypothermia for Ischemia in Near-Term Fetal Sheep." *Journal of Neuroinflammation* 19, no. 1: 139. https://doi.org/10.1186/s12974-022-02499-7.